**A Chiral Interlocking Auxiliary Strategy for the Synthesis of Mechanically Planar Chiral Rotaxanes**

Alberto de Juan,[#] David Lozano,[#] Andrew W. Heard,[+] Michael A. Jinks,[+] Jorge Meijide Suarez,[+] Graham J. Tizzard, and Stephen M. Goldup*

Chemistry, University of Southampton, Highfield, Southampton, SO17 1BJ (UK), *s.goldup@soton.ac.uk

[#]These authors contributed equally

[+]These authors contributed equally

**Abstract:** We have serendipitously discovered a combination of reaction partners that function as a "chiral interlocking auxiliary" to both orientate a macrocycle and, effectively, load it onto a new axle to generate mechanically planar chiral rotaxanes in high stereopurity (93-99% *ee*). We demonstrate the potential of the chiral interlocking auxiliary strategy through the synthesis of a number of targets in high enantiopurity, including so called "impossible" rotaxanes whose axles lack any functional groups that would allow their direct synthesis by other means. Intriguingly, by varying the order of bond forming steps, we can effectively choose which end of an axle the macrocycle is loaded onto, allowing the synthesis of both hands of a single target using the same reactions and building blocks.

## INTRODUCTION

The ability of the covalent subcomponents in mechanically interlocked molecules (MIMs)[1] to undergo large amplitude relative motion[2,3] is perhaps the most well-appreciated consequence of the mechanical bond. However, threading covalent fragments through one another to generate MIMs can also lead to molecular stereochemistry that relies solely on the mechanical bond[4,5,6], allowing MIMs to display molecular chirality even when their covalent subcomponents are achiral. However, the synthesis of enantiopure samples of such mechanically chiral molecules[7] has largely relied on chiral stationary phase HPLC (CSP-HPLC) separation of a racemic mixture of products[8,9,10], limiting the investigation of their properties.

To date, only two direct enantioselective syntheses of mechanically planar chiral (MPC) rotaxanes, molecules in which the stereochemistry relies on the combination of an axle that lacks mirror planes perpendicular to its principle axis and an "oriented" macrocycle whose only mirror plane lies parallel to the ring (Figure 1), have been reported[11,12]. Takata and co-workers reported the formation of

MPC enantiomers in 4.4% *ee* through the dynamic kinetic resolution of a pseudo-rotaxane precursor[11]. Leigh and co-workers recently reported a direct enantioselective synthesis of a MPC rotaxane under substrate control in an impressive 50% *ee* using their organocatalytic active template[13] reaction[14] in conjunction with a chiral alcohol leaving group[12]. Such direct enantioselective approaches are extremely attractive but, unless ~90% *ee* or higher can be achieved, the enantiomeric products still require CSP-HPLC separation for use in applications such as catalysis[15], sensing[10,16], and materials science[17]. Most recently, Kawabata and co-workers reported an elegant catalytic enantioselective kinetic resolution of a single mechanically planar chiral rotaxane that meets this requirement (>99% *ee* of unreacted starting material, 29% isolated yield), suggesting that such "classical" stereoselective synthetic methods warrant further investigation[18].

An alternative approach to enantiopure mechanically chiral MIMs that can circumvent the need for CSP-HPLC separation is to use a chiral auxiliary[19]. Including an enantiopure fixed covalent stereogenic unit in the MIM structure can give rise to an unequal mixture of diastereomers that differ in the configuration of the mechanical stereogenic unit[20,21]. Where required, these diastereomers can be separated using standard synthetic techniques prior to removal of the covalent stereogenic unit to provide enantioenriched mechanically chiral products in which the mechanical bond provides the sole source of stereochemistry. We have demonstrated this concept in the stereoselective synthesis of enantiopure MPC rotaxanes[20] and related topologically chiral catenanes[21]. However, although our auxiliary approach has allowed us to demonstrate the use of MPC rotaxanes in enantioselective Au-mediated catalysis[15]. the diastereoselectivity of the key mechanical bond forming step can vary significantly with the same auxiliary depending on the coupling partners used[20]. Furthermore, the separation of the mechanical epimers produced in the mechanical bond forming step is far from simple or assured, making high diastereoselectivity in the mechanical bond forming step extremely desirable.

Here we report the serendipitous discovery of a structural motif that functions both as a *chiral* auxiliary, to select the orientation of a macrocycle on an axle, and an *interlocking* auxiliary, to effectively allow the oriented macrocycle to be threaded selectively onto a new axle (Figure 1). We use this motif to

demonstrate the potential of a new “chiral interlocking auxiliary” strategy for the synthesis of MPC rotaxanes in excellent enantiopurity (93 - 99% *ee*), including so-called “impossible” rotaxanes, and functionalized examples through late-stage diversification. Furthermore, by effectively selecting which end of an axle the macrocycle is threaded onto, we demonstrate the synthesis of both hands of a target using the same building blocks, highlighting an intrinsic link between mechanical motion and mechanical stereochemistry.

**Figure 1.** The “chiral interlocking auxiliary” concept in the synthesis MPC rotaxanes

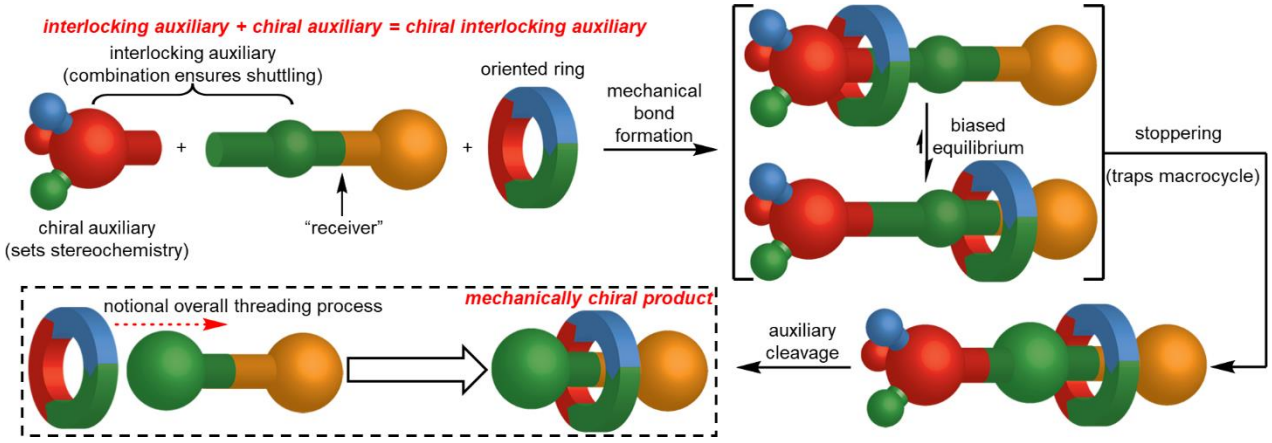


## RESULTS AND DISCUSSION

### Discovery of a potential chiral interlocking auxiliary motif

We previously demonstrated that amino acid-derived azide **1** can be used to generate MPC rotaxanes in up to 96% *de*, resulting in an overall 96% *ee* once the covalent stereogenic unit had been erased, using an active template copper-mediated alkyne-azide cycloaddition (AT-CuAAC)[22] strategy.[20] However, the stereoselectivity achieved with **1** varies considerably depending on the alkyne coupling partner used. Previously, preliminary computational modelling suggested that maximizing steric hindrance around the acetylene unit is key to achieving a high stereoselectivity[20]. Thus, we decided to compare the reaction of (*S*)-**1** (>99% *ee*, see Figure S1) in the presence of macrocycle **2** with alkynes **3a** and **3b** (Figure 2a).

**Figure 2.** (a) Synthesis of rotaxanes **4**.[a,b] (b) Partial $^1$H NMR ($CDCl_3$, 400 MHz, 298 K) of (i) the non-interlocked axle of rotaxane **4a**, (ii) rotaxane **4a**,[c] (iii) rotaxane **4b**,[d] (iv) the non-interlocked axle of rotaxane **4b** (colors and atom labels as in (a) with the exception of macrocycle protons which are shown in blue and the $CDCl_3$ peak which is light grey; correlations shown for protons $H_{trz}$, $H_{ether}$ and aliphatic protons derived from the azide unit). (c) Solid state structure of *rac*-**4b** in sticks and spacefilling representations with selected intercomponent interactions indicated (substituted benzyl ether unit omitted for clarity, colors as in (a), O, N and H atoms in dark grey, dark blue and white respectively).

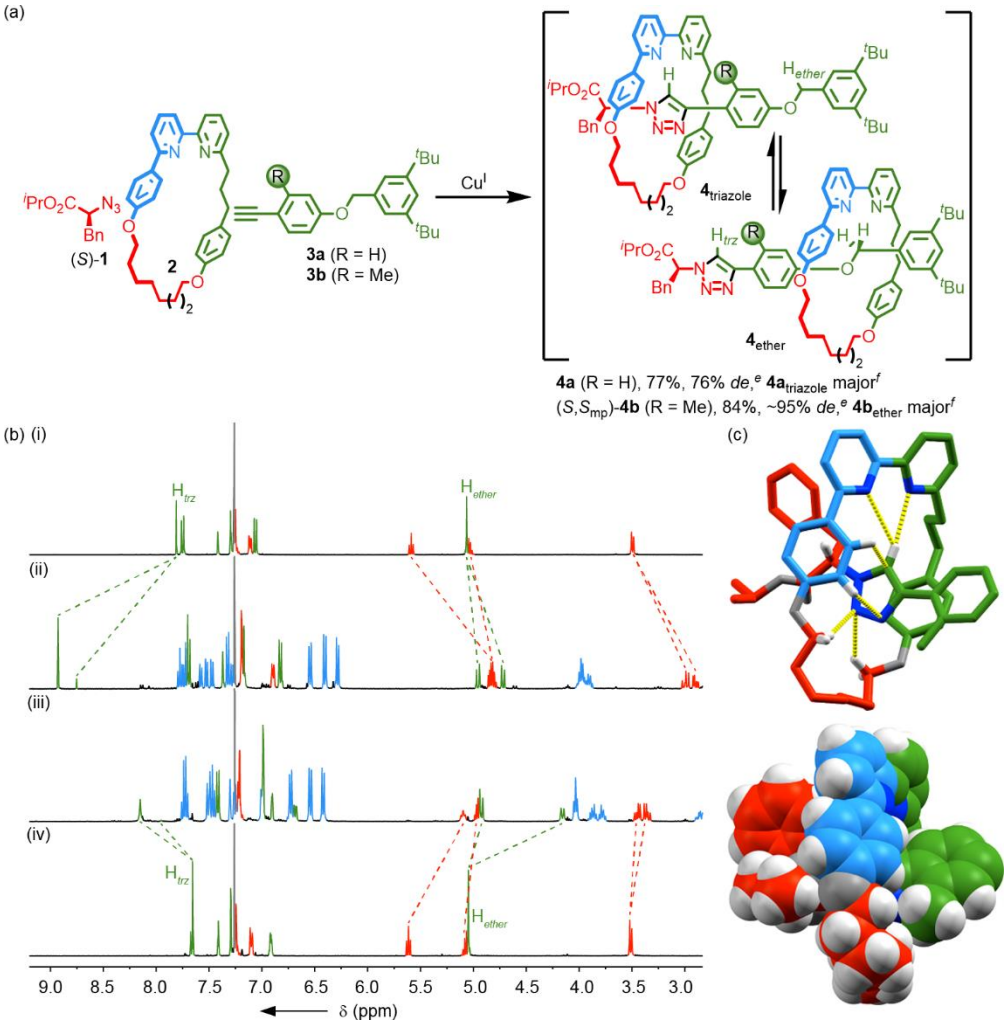


[a]Reagents and conditions: (*S*)-**1**, **2**, **3**, $[Cu(MeCN)_4]PF_6$, $^iPr_2EtN$, $CH_2Cl_2$, rt, 16 h (**4a**: 77%, 76% de; **4b**: 84%, ~95% *de*). [b]The absolute stereochemistry shown for rotaxanes **4** corresponds to the major ($S$,$S_{mp}$) isomer of **4b** determined by X-ray diffraction analysis. The major isomer of rotaxane **4a** was not determined. [c]Signals associated with the major stereoisomer are color coded, signals attributable to the minor stereoisomer are present but not assigned. [d]Rotaxane **4b** is contaminated with a small amount of the non-interlocked axle (4%) that we could not remove, as well as the minor diastereomer (~2%), which together account for the additional signals observed. [e]Determined by $^1$H NMR analysis of the crude reaction products (Figures S14 and S22). [f]Determined by $^1$H NMR analysis of the purified products (Table S2).

Alkyne **3a** gave rise to rotaxane **4a** in good yield but poor stereoselectivity (76% *de*), which could be assessed readily by $^1$H NMR analysis of the crude reaction product; two resonances were observed for triazole proton $H_{trz}$ at 8.93 and 8.75 ppm that were attributable to the major and minor mechanical epimers respectively (Figure 2bii). Both resonances appear at higher ppm than the corresponding signal of the non-interlocked axle (Figure 2bi, $\Delta\delta$ = 1.2 ppm for the major isomer), presumably due to a C-H•••N H-bond between the bipyridine Ns and $H_{trz}$, as is commonly observed in similar systems[23,24,25,26]. Pleasingly, consistent with our original hypothesis, reaction of more sterically hindered *o*-Me acetylene half-axle **3b** produced rotaxane **4b** in a significantly enhanced stereoselectivity (~95% *de*) and good isolated yield (84%). Indeed, to assign the diastereoselectivity of the reaction, samples of rotaxane **4b** had to be epimerized so that the $^1$H NMR resonances of the minor isomer could be identified (Figures S31-33).

Inspection of the $^1$H NMR spectrum of **4b** (Figure 2biii) led to two observations. Firstly, the resonance attributable to $H_{trz}$ appears much closer to that of the same proton in the corresponding axle (Figure 2biv, $\Delta\delta$ = 0.5 ppm) than observed for rotaxane **4a**. Secondly, the diastereotopic methylene ether protons, $H_{ether}$, appear as a well separated ($\Delta\delta$ = 0.7 ppm) pair of doublets in the $^1$H NMR spectrum of **4b**, whereas in the case of **4a** a much smaller separation was observed ($\Delta\delta$ = 0.2 ppm). This suggests that the mechanical stereochemistry of rotaxanes **4** is well expressed around the ether methylene unit (the same signals in the corresponding axles appear as a singlet) and that this effect is larger for **4b** than **4a**. In contrast, aliphatic protons derived from the azide component are more shielded in rotaxane **4a** than **4b** relative to the corresponding non-interlocked axle.

Taken together, these observations are consistent with rotaxanes **4** existing as a mixture of rapidly exchanging co-conformations in which the macrocycle is localized around either the triazole ($\mathbf{4}_{triazole}$) or ether ($\mathbf{4}_{ether}$) moiety of the axle (Figure 2a), presumably in both cases through C-H•••N H-bonds, augmented by other weak interactions ($\pi$-$\pi$, CH-$\pi$). Indeed, by comparing the difference in the $H_{trz}$ chemical shift of the corresponding non-interlocked axles and rotaxanes **4a** ($\Delta\delta$ = 1.2 ppm) and **4b** ($\Delta\delta$ = 0.5 ppm) with the maximum expected chemical shift difference were $\mathbf{4}_{triazole}$ the sole occupied co-

conformation ($\Delta\delta$ = ~2.3 and 1.8 ppm respectively, estimated by considering similar molecules in which the macrocycle is trapped around the triazole unit, see ESI for more details) suggests that **4a**$_{triazole}$ is slightly preferred (~52%) whereas **4b**$_{ether}$ is favored significantly (~72%).

The observed difference in co-conformational preference is presumably due to steric clash between the *o*-Me substituent and the ring which disfavors H-bonding to $H_{trz}$. X-ray diffraction analysis of single crystals obtained from a racemic sample of **4b** (synthesized by reaction of *rac*-**1**, **2** and **3b**) revealed solid state structures (two polymorphs were obtained that differ in their packing but are otherwise extremely similar; see Figures S378 and S379) consistent with this proposal. Although the **4b**$_{triazole}$ co-conformation was observed in the solid state (Figure 2c), the C-H•••N contacts are estimated to be longer than those in other otherwise similar systems[20] (C-H•••N = 2.6 and 3.0 *vs* 2.5 and 2.7 Å). The space filling representation of the solid-state structure also emphasizes the sterically crowded nature of the triazole unit as the macrocycle is seen to be buttressed on one side by the sterically crowded covalent stereogenic center and on the other by the *o*-Me substituent of the aryl unit. The unit cell of the crystals (both polymorphs) obtained from *rac*-**4b** contain a 1 : 1 ratio of ($R$,$R_{mp}$)-**4b** and ($S$,$S_{mp}$)-**4b**. HPLC analysis confirmed that the crystals analyzed correspond to the major diastereomer observed in a bulk sample of *rac*-**4b** (Figure S376, see ESI section S9 for full details). Thus the solid-state structures obtained from *rac*-**4b** allowed us to assign the absolute stereochemistry of the major isomer obtained from the reaction of (*S*)-**1**, **2** and **3b** to be ($S$,$S_{mp}$)-**4b**.

An "interlocking auxiliary", as introduced by Leigh and co-workers[27] and recently extended by Coutrot[28], is a unit that facilitates mechanical bond formation but from which the macrocycle can then be shuttled away readily to a "receiver" region of the axle (Figure 1). The macrocycle is then trapped in this co-conformation by chemical modification of the axle before the interlocking auxiliary unit is removed. Based on the results above, the combination of azide **1** with an *o*-Me aromatic alkyne appears to meet the requirements of both a chiral auxiliary (high stereoselectivity) and interlocking auxiliary (weak non-covalent interactions with the functional group produced) and so could combine these functions as a "chiral interlocking auxiliary".

**Demonstration of the chiral interlocking auxiliary concept**

To validate our hypothesis, we investigated the AT-CuAAC reaction of *o*-Me alkyne **5a** with azide (*S*)-**1** and macrocycle **2** with the intention of shuttling the macrocycle onto the unhindered triazole unit prior to removing the chiral interlocking auxiliary to generate rotaxane **8**. AT-CuAAC coupling of **5a** with (*S*)-**1** and **2** gave rotaxane **6** in high isolated yield (80%). $^1$H NMR analysis of **6** (Figure S51) suggests that, as expected, the macrocycle is significantly displaced from the hindered triazole; $H_{trz}$ of the auxiliary unit appears at relatively low chemical shift ($\delta$ = 7.60 ppm) and the diastereotopic benzylic methylene protons appear as a well separated pair of doublets ($\Delta\delta$ = 0.58 ppm). We were unable to ascertain the diastereopurity of **6** at this stage as only one set of signals could be observed clearly. The PMB group was removed to give rotaxane **7** in which the ring is free to shuttle to the unhindered triazole. Reaction with $TMSCHN_2$ "stoppered" the new axle, trapping the macrocycle over the receiver unit. Finally, addition of $K_2CO_3$ and MeOH removed the auxiliary fragment to give a crude reaction product containing rotaxane **8** and macrocycle **2** in a 96 : 4 ratio, as judged by $^1$H NMR analysis of the crude reaction mixture (Figure S58), suggesting that, as expected, the macrocycle is significantly displaced towards the unhindered triazole unit of the receiver unit of rotaxane **7** under the reaction conditions.

Overall, rotaxane **8** was isolated in 65% yield over 3 chemical steps from **6** (52% from half-axle **5a**). Alternatively, starting from carboxylic acid half-axle **5b**, rotaxane **7** could be produced directly in the AT-CuAAC coupling and converted to rotaxane **8** in 61% yield over 3 chemical steps from **5b** without isolation of the intermediate structures. CSP-HPLC analysis of the samples of rotaxane **8** produced using our chiral interlocking auxiliary strategy revealed an enantiopurity of 97% *ee*, suggesting that the initial AT-CuAAC coupling proceeds in ~97% *de* (it should be noted that, because the two diastereomers may have different co-conformational preferences, the link between the *de* of the initial coupling and the *ee* of the final product is not direct or simple; see ESI section S7 for details). Given that the *para* substituent of the acetylene moiety appears not to strongly influence the diastereoselectivity of the process (both **4b** and **8** are produced with similar stereopurity), it is reasonable to assume the orientation of the macrocycle on the axle is the same in both cases. Thus, we tentatively assign the dominant configuration of **8** to be

($S_{mp}$)-**8** and by extension, the intermediates to be ($S$,$S_{mp}$)-**6** and ($S$,$S_{mp}$)-**7**. Although we are confident in this assumption, further work to validate the stereoisomer produced using spectroscopic means are ongoing[29].

**Figure 3.** (a) A chiral interlocking auxiliary synthesis of MPC rotaxane ($S_{mp}$)-**8** using an esterification stoppering strategy.[a] (b) A chiral interlocking auxiliary synthesis of MPC rotaxane ($S_{mp}$)-**10** using a cross-coupling stoppering strategy.[b] (c) A chiral interlocking auxiliary synthesis of phosphine oxide-containing MPC rotaxane ($S_{mp}$)-**12**.[c]

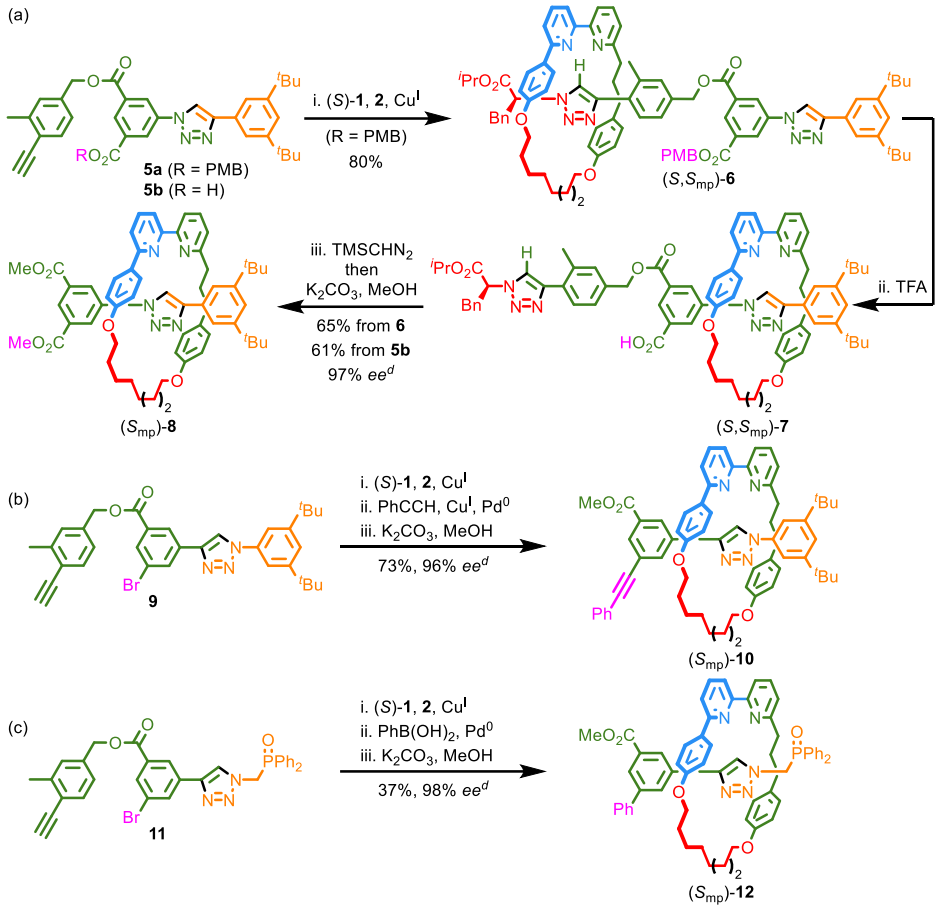


[a]Reagents and conditions: i. (*S*)-**1**, **2**, **5a**, $[Cu(MeCN)_4]PF_6$, $^iPr_2EtN$, $CH_2Cl_2$, rt, 16 h (80%); ii. TFA, $CH_2Cl_2$, rt, 16 h; iii. $TMSCHN_2$ (2.0 M in hexanes), MeCN, rt, 16 h then MeOH, $K_2CO_3$, rt, 3 h (65% over two steps, 94% *ee*). [b]Reagents and conditions: i. (*S*)-**1**, **2**, **9**, $[Cu(MeCN)_4]PF_6$, $^iPr_2EtN$, $CH_2Cl_2$, rt, 16 h (89%); ii. PhCCH, $PdCl_2(PPh_3)_2$, CuI, $^iPr_2NH$, 110 °C, 16 h (94%); iii. $K_2CO_3$, MeOH, $CH_2Cl_2$, rt, 16 h (87%, 96% *ee*). [c]Reagents and conditions: i. (*S*)-**1**, **2**, **11**, $[Cu(MeCN)_4]PF_6$, $^iPr_2EtN$, $CH_2Cl_2$, rt, 16 h (85%); ii. $PhB(OH)_2$, $Pd(OAc)_2$, $PPh_3$, $K_3PO_4.H_2O$, THF, 80 °C, 16 h (93%); iii. $K_2CO_3$, MeOH, $CH_2Cl_2$, rt, 16 h (70%, 98% *ee*). [d]Determined by CSP-HPLC.

A key advantage of the chiral interlocking auxiliary concept is that, if the azide and *o*-Me aryl acetylene units are conserved (i.e. the chiral interlocking auxiliary component), other details of the structure and reaction sequence can be varied without significantly altering the outcome of the process. For example, if the protected ester functional group of **5a** is replaced by a bromine atom, a similar sequence can be performed in which the stoppering step is achieved using a $Pd^0$ mediated cross

coupling. Reaction of acetylene **9** with macrocycle **2** and azide (*S*)-**1** followed by Sonagashira coupling and transesterification to remove the interlocking auxiliary, gave rise to rotaxane ($S_{mp}$)-**10**, once again in good yield over 3 chemical steps from **9** (73%) and enantiopurity (96% *ee*). Similarly, it is relatively trivial to alter the structure of the receiver portion of the axle. Reaction of half-axle **11** with (*S*)-**1** and macrocycle **2**, followed by Suzuki cross coupling and cleavage of the auxiliary unit by transesterification, gave MPC phosphine oxide ($S_{mp}$)-**12** in 37% overall yield from **11** and excellent enantiopurity (98% *ee*). Finally, to demonstrate the importance of the *o*-Me group in determining the shuttling efficiency and stereoselectivity a sample of rotaxane ($S_{mp}$)-**10** was produced using an analogue of alkyne **9** (compound **S87**, see ESI section S8 for details) that lacked this key functionality. As expected, using this approach, rotaxane ($S_{mp}$)-**10** was produced in diminished enantiopurity (83% *ee*) and analysis of the crude product of transesterification revealed significant quantities of non-interlocked macrocycle **2** (78 : 22 ($S_{mp}$)-**10** : **2**), which was not observed when alkyne **9** was used (96 : 4).

**Synthesis of "impossible" MPC rotaxanes using a chiral interlocking auxiliary strategy**

The results above demonstrate that the combination of azide **1** and an *o*-Me aryl acetylene benzylic ester fragment can act as a chiral interlocking auxiliary with macrocycle **2**. However, rotaxanes **8**, **10** and **12** can all be synthesized directly using the AT-CuAAC reaction, albeit in racemic form. Given that one of the benefits of the interlocking auxiliary concept is that it allows access to targets that do not contain motifs that facilitate mechanical bond formation, we set out to explore the limits of our methodology through the synthesis of such so-called "impossible rotaxanes", molecules in which there is no significant interaction between axle and macrocycle (Figure 4).

Using a precursor analogous to alkyne **5a** but in which the triazole receiving unit is replaced with a simple alkyl bis-ether fragment gave rotaxane ($S_{mp}$)-**13** (Figure 4a, see ESI for more detail). In this case the macrocycle is presumed to interact with the receiving unit through C-H•••N hydrogen bonds between the polarized ether protons and the bipyridine unit. Despite the comparatively weak nature of these interactions, $^1$H NMR analysis of the crude reaction mixture after transesterification revealed an 88 : 12 ratio of rotaxane ($S_{mp}$)-**13** to macrocycle **2** (Figure S160), compared with the 96 : 4 ratio of product to

macrocycle **2** observed in the case of ($S_{mp}$)-**8** (Figure S58), suggesting that the co-conformation in which the macrocycle encircles the ether unit is still significantly preferred in the precursor to ($S_{mp}$)-**13**. Overall, rotaxane ($S_{mp}$)-**13** was isolated in 52% yield and 94% *ee* over 4 steps from the corresponding alkyne half-axle.

**Figure 4.** Synthesis of "impossible" MPC rotaxanes. (a) Rotaxanes ($S_{mp}$)-**13**-**15** synthesized using the esterification stoppering approach.[a] (b) Late-stage diversification of rotaxane ($S$,$S_{mp}$)-**17** to give MPC rotaxanes ($S_{mp}$)-**18**-**20** through a $Pd^0$-mediated stoppering approach.[b]

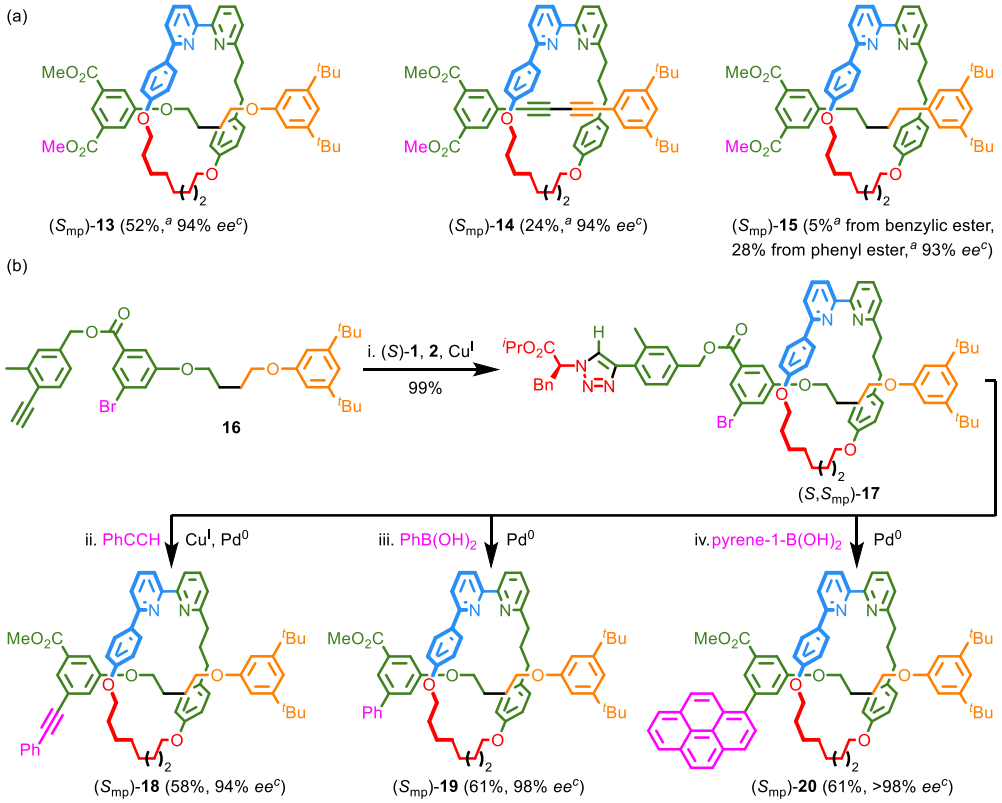


[a]The yields of rotaxanes ($S_{mp}$)-**13**-**15** refer to the overall isolated yield over 4 steps from the corresponding alkyne-PMB ester half-axle. Rotaxane ($S_{mp}$)-**15** was also synthesized over 3 steps from the corresponding alkyne-carboxylic acid half-axle (yield given). [b]Reagents and conditions: i. (*S*)-**1**, **2**, **16**, $[Cu(MeCN)_4]PF_6$, $^iPr_2EtN$, $CH_2Cl_2$, rt, 16 h (99%); ii. PhCCH, $PdCl_2(PPh_3)_2$, CuI, $^iPr_2NH$, 110 °C, 16 h, (aqueous work up), then MeOH, $K_2CO_3$, $CH_2Cl_2$, rt, 16 h (58%, 94% *ee*); iii. $PhB(OH)_2$, $Pd(OAc)_2$, $PPh_3$, $K_3PO_4.H_2O$, THF, 80 °C, 16 h (aqueous work up), then MeOH, $K_2CO_3$, $CH_2Cl_2$, rt, 16 h (61%, 98% *ee*); iv. Pyrene-1-$B(OH)_2$, $Pd(OAc)_2$, $PPh_3$, $K_3PO_4.H_2O$, THF, 80 °C, 16 h (aqueous work up), then MeOH, $K_2CO_3$, $CH_2Cl_2$, rt, 16 h (61%, >98% *ee*; no trace of the other enantiomer was observed by CSP-HPLC. However, baseline separation could not be achieved and thus we assign the *ee* as >98%.). [c]Determined by CSP-HPLC.

To probe the effect of reducing the strength of the interactions between the receiving unit and the macrocycle further, we synthesized rotaxane ($S_{mp}$)-**14** in which the diyne receiving unit presents no significant attractive interactions to the macrocycle. Surprisingly, the crude product mixture after transesterification revealed a ratio of ($S_{mp}$)-**14** : **2** of ~43 : 57 (Figure S183), allowing rotaxane ($S_{mp}$)-**14**

(94% *ee*) to be isolated in 24% overall yield from the corresponding alkyne half-axle. Similarly, rotaxane ($S_{mp}$)-**15**, in which the macrocycle encircles a simple alkyl chain could be synthesized, albeit in a much lower isolated yield of just 13% in the final step (5% from the corresponding alkyne half-axle). The low yield of ($S_{mp}$)-**15** is due in part to challenging purifications at all stages of the synthesis. In this case, the synthesis of ($S_{mp}$)-**15** could be improved by using a phenolic ester link between the auxiliary and the receiver unit in place of the benzylic ester and completing the synthesis without purification of the intermediates (See ESI Section S4.4 for details). Using this approach, rotaxane ($S_{mp}$)-**15** was isolated in 28% yield over 3 steps from the corresponding alkyne half-axle. In both routes, whether using the benzylic ester or phenolic ester, the ratio between product and non-interlocked macrocycle in the crude reaction mixture after transesterification observed by $^1$H NMR was ~ 40 : 60 (Figures S215 and S223).

Finally, we extended our synthesis of impossible MPC rotaxanes by demonstrating the use of our $Pd^0$-mediated cross-coupling stoppering approach in the late-stage diversification of a common building block.[30] Rotaxane (*S*,$S_{mp}$)-**17** was synthesized from alkyne half-axle **16** by reaction with macrocycle **2** and azide (*S*)-**1** in excellent yield (99%). (*S*,$S_{mp}$)-**17** was then subjected to different $Pd^0$-mediated cross-coupling reactions followed by transesterification to remove the auxiliary; Sonagashira cross-coupling with phenyl acetylene gave conjugated rotaxane ($S_{mp}$)-**18**, Suzuki cross-coupling with $PhB(OH)_2$ gave ($S_{mp}$)-**19**, and Suzuki cross-coupling with pyrene-1-boronic acid gave rotaxane ($S_{mp}$)-**20** all in good yield and enantiopurity (≥94% *ee* in all cases).

**Stereodivergent synthesis using a grafting approach and a single set of building blocks**

Our chiral interlocking auxiliary strategy notionally achieves the threading of a macrocycle onto an axle in a fixed orientation (Figure 1). Perhaps less obviously, if a single auxiliary unit is used, the absolute configuration of the final product depends on which end of the receiver unit the auxiliary is connected to. Thus, in theory, it is possible to synthesize both enantiomers of an MPC rotaxane using a single stereoisomer of the auxiliary by selecting which side the ring is threaded from.

To demonstrate this principle, we extended our chiral interlocking auxiliary approach to employ a direct aminolysis reaction to remove the auxiliary unit, which avoids the need for a stoppering step to trap the macrocycle on the receiver region, a so-called "grafting"[28,31] approach (Figure 5a). Precursor **21a** was produced in 80% yield by reaction of the corresponding alkyne with azide (*S*)-**1** and macrocycle **2** (see ESI). The macrocycle in **21a** is free to explore the length of the axle and, as expected, $^1$H NMR analysis suggested the preferred co-conformation is that in which the ring encircles the alkyl chain of the ester portion of the axle ($\delta(H_{trz})$ = 8.00 ppm, consistent with **21a**$_{trz}$ : **21a**$_{ester}$ ~ 1 : 10), where it presumably engages in C-H•••N H-bonding interactions. Reaction of **21a** with benzylamine **22a** gave rotaxane **23a** with good selectivity for the interlocked product; a ratio of 83 : 17 (**23a** : **2**) was observed by $^1$H NMR analysis of the crude aminolysis reaction product (Figure S284). $^1$H NMR analysis of **23a** suggests that the macrocycle engages in an N-H•••N H-bond with the amide proton of the axle as this signal appears at a high chemical shift ($\delta$(NH) = 8.22 ppm, Figure S285).

It is noteworthy that when a shorter alkyl ester receiver unit was used (**21b**) the aminolysis reaction proceeded more slowly than that of **21a** and with very poor selectivity for the interlocked product (**23b** : **2** ~ 4 : 96, Figure S302), despite $^1$H NMR analysis of **21b** also suggesting that the preferred co-conformation of **21b** is that in which the ring encircles the receiver portion of the axle ($\delta(H_{trz})$ = 8.00 ppm). We tentatively attribute the poor selectivity for **23b** to an unfavorable kinetic resolution process; as the phenolic ester unit is much more hindered when the macrocycle occupies the receiver unit (**21**$_{ester}$), the reaction preferentially occurs when the ring occupies the less favorable triazole binding site (**21**$_{triazole}$). Thus, although the direct aminolysis grafting approach provides a synthetically simple route to MPC rotaxanes as it removes the need for a separate stoppering step, it is more prone to steric effects, as might be expected given that the macrocycle is proximal to the reacting ester functionality in the key step (see ESI section S7 for a more detailed discussion of the role of co-conformational bias and reaction rates in an interlocking auxiliary syntheses).

**Figure 5.** (a) Chiral interlocking auxiliary synthesis of MPC rotaxanes ($S_{mp}$)-**23** using an aminolysis grafting reaction.[a] (b) Synthesis of both enantiomers of MPC rotaxane **28** by varying the order of amide bond forming steps.[b]

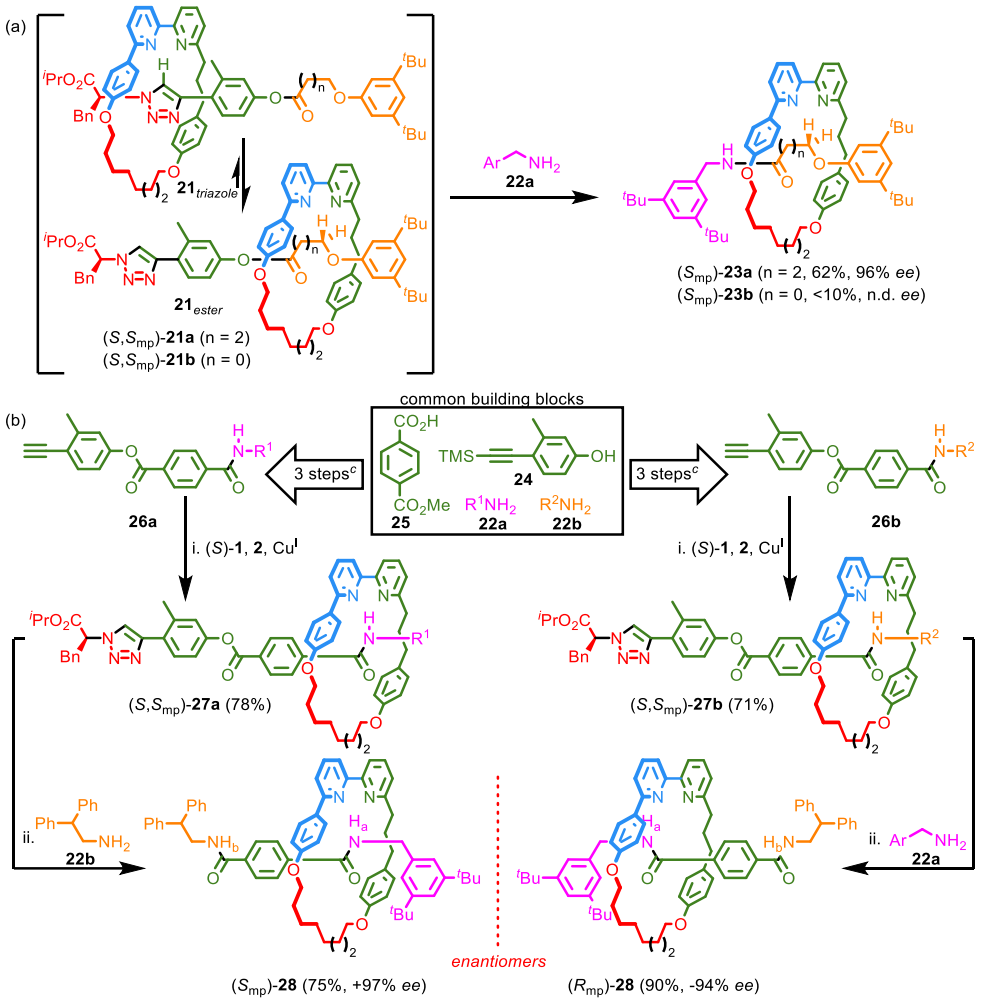


[a]Reagents and conditions: **22a** (Ar = 3,5-$^t$BuC$_6$H$_3$), $CH_2Cl_2$, 60 °C, 16 h (**23a**: 62%, 96% *ee*; **23b**: <10%, *ee* n.d.). [b]Reagents and conditions: i. (*S*)-**1**, **2**, **26**, [Cu(MeCN)$_4$]PF$_6$, $^i$Pr$_2$EtN, $CH_2Cl_2$, rt, 16 h ((*S*,*S*$_{mp}$)-**27a**: 78%; (*S*,*S*$_{mp}$)-**27b**: 71%); ii. **22**, $CH_2Cl_2$, 60 °C, 16 h ((*S*$_{mp}$)-**28**: 75%, 98% *ee*; (*R*$_{mp}$)-**28**: 90%, 94% *ee*). [c]See ESI for details.

Having developed this simple aminolysis approach, we turned our attention to synthesizing both enantiomers of rotaxane **28** by making use of common axle building blocks alkyne **24**, carboxylic acid **25**, and amines **22** (Figure 5b). Coupling of **25** with amine **22a** followed by ester hydrolysis, ester formation by reaction with **24** and removal of the TMS unit gave half-axle **26a**. AT-CuAAC coupling of **26a** with azide (*S*)-**1** and macrocycle **2** gave rotaxane (*S*,*S*$_{mp}$)-**27a**. Aminolysis of (*S*,*S*$_{mp}$)-**27a** with amine **22b** gave rotaxane (*S*$_{mp}$)-**28**. If instead carboxylic acid **25** was coupled first with amine **22b** and the same sequence followed finishing with aminolysis by amine **22a**, the opposite enantiomer of the product, (*R*$_{mp}$)-**28**, was produced as the major product. Circular dichroism (CD) and CSP-HPLC analysis of the products

of these two sequences reveal mirror image spectra (Figure 6a) and enantiopurities of ≥|94%| *ee* (Figure 6b) for both routes. In both cases, the interlocked product is the major species observed after the grafting reaction; $^{1}$H NMR analysis of the crude reaction products revealed a ratios of 98 : 2 and 97 : 3 rotaxane : macrocycle for ($S_{mp}$)-**28** and ($R_{mp}$)-**28** respectively (Figures S317, S341). $^{1}$H NMR analysis of rotaxane **28** suggests that the macrocycle shuttles between and interacts with both amide protons of the axle as the corresponding signals appear at chemical shifts ($\delta(NH_a)$ ~ 7.7 ppm, $\delta(NH_b)$ ~ 7.1 ppm, Figure S319) intermediate between those of the non-interlocked axle ($\delta(NH_a)$ = 6.3 ppm, $\delta(NH_b)$ ~ 6.1 ppm, Figure S345) and the equivalent protons of precursors **27a** (9.2 ppm, Figure S311) and **27b** (8.7 ppm, Figure S335).

**Figure 6.** (a) Circular dichroism spectra of the enantiomers of rotaxane **28**.[a] (b) CSP-HPLC analysis of ($R_{mp}$)-**28** (+98% *ee*) and ($S_{mp}$)-**28** (-94% *ee*).[b]

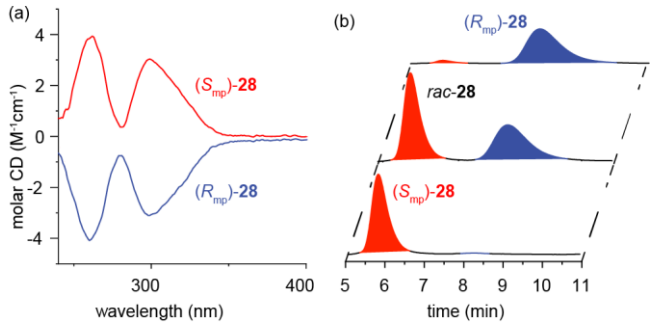


[a]Measured in $CHCl_3$ (46 and 44 mM for ($S_{mp}$)-**28** and ($R_{mp}$)-**28** respectively, 10 mm path length, 293 K). [b]RegisCell, *n*-hexane-EtOH 80 : 20 (1.0 $mLmin^{-1}$).

## CONCLUSIONS

In conclusion, we have demonstrated a new chiral interlocking auxiliary strategy for the synthesis of MPC rotaxanes in which the mechanical bond provides the only stereogenic unit using the AT-CuAAC reaction of a simple α-chiral azide and an *o*-Me-aromatic acetylene. We demonstrate the synthetic power of the chiral interlocking auxiliary concept through the synthesis of challenging MPC rotaxanes in excellent (≥93% *ee*) enantiopurity, including “impossible” rotaxanes where, for example, the macrocycle encircles a simple alkyl chain (rotaxane **15**, Figure 4). By employing a cross-coupling reaction as the stoppering step, late-stage diversification of a single rotaxane building block was also achieved.[30] We also demonstrated an unusual property of combining molecular motion and mechanical chirality, namely the

potential to synthesize both hands of an MPC target using the same starting materials by controlling which end of the axle the macrocycle is effectively threaded on from.

Although to date the AT-CuAAC reaction has proved particularly useful for the synthesis of mechanically chiral molecules,[7] in principle the chiral interlocking auxiliary concept is not limited to any single mechanical bond forming reaction or template; it should be possible to extend this strategy to other mechanical bond forming approaches by identifying a covalent chiral unit that gives rise to diastereoselective mechanical bond formation and from which the macrocycle can be shuttled away. However, there are some practical issues to be considered. Firstly, we anticipate that some degree of optimization will be required for each macrocycle used as the interactions between the macrocycle and auxiliary determine both the efficiency of the mechanical bond formation (yield and diastereoselectivity), and the co-conformational behavior of the product. Indeed, varying the size of macrocycle **2** employed in the reaction of (*S*)-**1** and **3b** by removing or adding a methylene unit to the ether linker (see ESI section S10 for details) resulted in a reduced selectivity for mechanical bond formation in the case of the smaller macrocycle (45%, ~92% de), whereas in the case of the larger ring high selectivity for mechanical bond formation was observed but the stereoselectivity of the reaction was somewhat reduced (87%, 90% *de*). In both cases, $^{1}$H NMR analysis suggests that the macrocycle appears to be displaced from the hindered triazole in the product. Thus, although the stereoselectivities and yield of mechanical bond formation obtained with these modified macrocycles remains useful, the chiral interlocking auxiliary represented by the o-Me acetylene unit and azide **1** appears to perform best with macrocycle **2**. Another practical concern in the development of new chiral interlocking auxiliary strategies is that the co-conformational bias between auxiliary and receiver, which plays a significant role in the yield of the process, is potentially dependent on the stoppering reaction conditions employed. For example, rotaxane **13** (Figure 4) is produced in ~9 : 1 ratio with macrocycle **2** using the esterification stoppering strategy, which is similar to the co-conformational bias observed by $^{1}$H NMR ($CDCl_3$, 298 K) for rotaxane **17**. However, stoppering rotaxane **17** using cross-coupling reactions to give rotaxanes **18**-**20** results in a product mixture

containing rotaxane and macrocycle **2** in a ~63 : 37 ratio, suggesting that the co-conformational preference of **17** is significantly altered under the reaction conditions. Finally, it is essential that the auxiliary is not cleaved under the conditions of the stoppering reaction, at least before the reaction is complete, and even then the synthesis will only be viable if the product of cleavage is itself a [2]rotaxane (i.e. the stoppers are big enough to prevent the ring escaping).

These practical considerations notwithstanding, as clearly demonstrated here, once an optimized chiral interlocking auxiliary system is established it can be used to synthesise a wide range of rotaxanes based on a given macrocycle efficiently in reliably excellent enantiopurity, something that has not proved possible with simple chiral auxiliaries.[15,20] Given recent reports of applications of mechanically chiral molecules[10,15,17,32,33], and the increasing interest in the applications of chiral interlocked molecules in general[34,35,36,37,38,39], we anticipate that these findings will spur further progress in the development of functional mechanically chiral systems.

**ACKNOWLEDGEMENTS**

SMG thanks the European Research Council (Consolidator Grant Agreement no. 724987), EPSRC (EP/L016621/1) and Leverhulme Trust (ORPG-2733) for funding and the Royal Society for a Wolfson Research Fellowship. JMS thanks the Royal Society for a Newton International Fellowship. AWH thanks the University of Southampton for a Presidential Scholarship.

**DATA AVAILABILITY**

Crystallographic data for rotaxane *rac*-**4b** have been deposited at the Cambridge Crystallographic Data Centre (http://www.ccdc.cam.ac.uk/) under CCDC number 2069804. These data can be obtained free of charge via https://www.ccdc.cam.ac.uk/structures/. All other data supporting the findings of this study are available within the paper and its Supplementary Information.

**CONTRIBUTIONS**

MAJ synthesized rotaxane **4b**. MAJ and AdJ developed the chiral interlocking auxiliary concept in collaboration with SMG. AdJ synthesized rotaxanes **8**, **13**-**15**, **23** and **28** with support from MAJ who provided synthetic intermediates. DL performed the stereochemical characterization of rotaxanes **4**, **8**, **13**-**15**, **23** and **28.** DL carried out the co-conformational analysis of rotaxane **4** and associated experiments. AWH and JMS developed the cross-coupling concept and collaborated to synthesize rotaxane **10**. JMS synthesized and characterized rotaxanes **18**-**20** and demonstrated the importance of the *o*-Me group using alkyne **S87**. AWH synthesized and characterized rotaxane **12**. GJT collected the single-crystal x-ray diffraction data of rac-**4b** and solved and refined the structure. DL and AWH managed the preparation of the Supporting Information. SMG directed the research. All authors contributed to the analysis of the results and the writing of the manuscript.

**REFERENCES**

(1) Bruns, C. J. & Stoddart, J. F. *The Nature of the Mechanical Bond: From Molecules to Machines*. (Wiley, 2016).

(2) Erbas-Cakmak, S., Leigh, D. A., McTernan, C. T. & Nussbaumer, A. L. Artificial Molecular Machines. *Chem. Rev.* **115**, 10081-10206 (2015).

(3) Heard, A. W. & Goldup, S. M. Simplicity in the Design, Operation, and Applications of Mechanically Interlocked Molecular Machines. *ACS Cent. Sci.* **6**, 117-128 (2020).

(4) Jamieson, E. M. G., Modicom, F. & Goldup, S. M. Chirality in rotaxanes and catenanes. *Chem. Soc. Rev.* **47**, 5266-5311 (2018).

(5) Evans, N. H. Chiral Catenanes and Rotaxanes: Fundamentals and Emerging Applications. *Chem. Eur. J.* **24**, 3101-3112 (2018).

(6) Nakazono, K. & Takata, T. Mechanical Chirality of Rotaxanes: Synthesis and Function. *Symmetry* **12** (2020).

(7) Maynard, J. R. J. & Goldup, S. M. Strategies for the Synthesis of Enantiopure Mechanically Chiral Molecules. *Chem* **6**, 1914-1932 (2020).

(8) Kaida, Y., Okamoto, Y., Chambron, J. C., Mitchell, D. K. & Sauvage, J. P. The Separation of Optically-Active Copper (I) Catenates. *Tetrahedron Lett.* **34**, 1019-1022 (1993).

(9) Yamamoto, C., Okamoto, Y., Schmidt, T., Jager, R. & Vogtle, F. Enantiomeric resolution of cycloenantiomeric rotaxane, topologically chiral catenane, and pretzel-shaped molecules: Observation of pronounced circular dichroism. *J. Am. Chem. Soc.* **119**, 10547-10548 (1997).

(10) Hirose, K., Ukimi, M., Ueda, S., Onoda, C., Kano, R., Tsuda, K., Hinohara, Y. & Tobe, Y. The Asymmetry is Derived from Mechanical Interlocking of Achiral Axle and Achiral Ring Components - Syntheses and Properties of Optically Pure [2]Rotaxanes-. *Symmetry* **10**, 20 (2018).

(11) Makita, Y., Kihara, N., Nakakoji, N., Takata, T., Inagaki, S., Yamamoto, C. & Okamoto, Y. Catalytic Asymmetric Synthesis and Optical Resolution of Planar Chiral Rotaxane. *Chem. Lett.* **36**, 162-163 (2007).

(12) Tian, C., Fielden, S. D. P., Perez-Saavedra, B., Vitorica-Yrezabal, I. J. & Leigh, D. A. Single-Step Enantioselective Synthesis of Mechanically Planar Chiral [2]Rotaxanes Using a Chiral Leaving Group Strategy. *J. Am. Chem. Soc.* **142**, 9803-9808 (2020).

(13) Denis, M. & Goldup, S. M. The active template approach to interlocked molecules. *Nat Rev Chem* **1**, 0061 (2017).

(14) Tian, C., Fielden, S. D. P., Whitehead, G. F. S., Vitorica-Yrezabal, I. J. & Leigh, D. A. Weak functional group interactions revealed through metal-free active template rotaxane synthesis. *Nat. Commun.* **11**, 744 (2020).

(15) Heard, A. W. & Goldup, S. M. Synthesis of a Mechanically Planar Chiral Rotaxane Ligand for Enantioselective Catalysis. *Chem* **6**, 994-1006 (2020).

(16) Gaedke, M., Witte, F., Anhauser, J., Hupatz, H., Schroder, H. V., Valkonen, A., Rissanen, K., Lutzen, A., Paulus, B. & Schalley, C. A. Chiroptical inversion of a planar chiral redox-switchable rotaxane. *Chem. Sci.* **10**, 10003-10009 (2019).

(17) Ishiwari, F., Nakazono, K., Koyama, Y. & Takata, T. Induction of Single-Handed Helicity of Polyacetylenes Using Mechanically Chiral Rotaxanes as Chiral Sources. *Angew. Chem. Int. Ed.* **56**, 14858-14862 (2017).

(18) Imayoshi, A., Lakshmi, B. V., Ueda, Y., Yoshimura, T., Matayoshi, A., Furuta, T. & Kawabata, T. Enantioselective preparation of mechanically planar chiral rotaxanes by kinetic resolution strategy. *Nat Commun* **12**, 404 (2021).

(19) Eliel, E., Wilen, S. & Mander, L. *Stereochemistry of Organic Compounds*. (John Wiley and Sons, Inc., 1994).

(20) Jinks, M. A., de Juan, A., Denis, M., Fletcher, C. J., Galli, M., Jamieson, E. M. G., Modicom, F., Zhang, Z. & Goldup, S. M. Stereoselective Synthesis of Mechanically Planar Chiral Rotaxanes. *Angew. Chem. Int. Ed.* **57**, 14806-14810 (2018).

(21) Denis, M., Lewis, J. E. M., Modicom, F. & Goldup, S. M. An Auxiliary Approach for the Stereoselective Synthesis of Topologically Chiral Catenanes. *Chem* **5**, 1512-1520 (2019).

(22) Aucagne, V., Hanni, K. D., Leigh, D. A., Lusby, P. J. & Walker, D. B. Catalytic "click" rotaxanes: a substoichiometric metal-template pathway to mechanically interlocked architectures. *J. Am. Chem. Soc.* **128**, 2186-2187 (2006).

(23) Lahlali, H., Jobe, K., Watkinson, M. & Goldup, S. M. Macrocycle size matters: "small" functionalized rotaxanes in excellent yield using the CuAAC active template approach. *Angew. Chem. Int. Ed.* **50**, 4151-4155 (2011).

(24) Lewis, J. E. M., Modicom, F. & Goldup, S. M. Efficient Multicomponent Active Template Synthesis of Catenanes. *J. Am. Chem. Soc.* **140**, 4787-4791 (2018).

(25) Cirulli, M., Kaur, A., Lewis, J. E. M., Zhang, Z., Kitchen, J. A., Goldup, S. M. & Roessler, M. M. Rotaxane-Based Transition Metal Complexes: Effect of the Mechanical Bond on Structure and Electronic Properties. *J. Am. Chem. Soc.* **141**, 879-889 (2019).

(26) Zhang, Z., Tizzard, G. J., Williams, J. A. G. & Goldup, S. M. Rotaxane PtII-complexes: mechanical bonding for chemically robust luminophores and stimuli responsive behaviour. *Chem. Sci.* **11**, 1839-1847 (2020).

(27) Hannam, J. S., Lacy, S. M., Leigh, D. A., Saiz, C. G., Slawin, A. M. & Stitchell, S. G. Controlled submolecular translational motion in synthesis: a mechanically interlocking auxiliary. *Angew. Chem. Int. Ed.* **43**, 3260-3264 (2004).

(28) Chao, S., Romuald, C., Fournel-Marotte, K., Clavel, C. & Coutrot, F. A strategy utilizing a recyclable macrocycle transporter for the efficient synthesis of a triazolium-based [2]rotaxane. *Angew. Chem. Int. Ed.* **53**, 6914-6919 (2014).

(29) Koenis, M. A. J., Chibueze, C. S., Jinks, M. A., Nicu, V. P., Visscher, L., Goldup, S. M. & Buma, W. J. Vibrational circular dichroism spectroscopy for probing the expression of chirality in mechanically planar chiral rotaxanes. *Chem Sci* **11**, 8469-8475 (2020).

(30) Coutrot, F., Waeles, P. & Gauthier, M. Challenges and Opportunities in the Post-Synthetic Modification of Interlocked Molecules. *Angew. Chem. Int. Ed.* (2020).

(31) Rowan, S. J. & Stoddart, J. F. Precision Molecular Grafting: Exchanging Surrogate Stoppers in [2]Rotaxanes. *J. Am. Chem. Soc.* **122**, 164-165 (2000).

(32) Gaedke, M., Witte, F., Anhauser, J., Hupatz, H., Schroder, H. V., Valkonen, A., Rissanen, K., Lutzen, A., Paulus, B. & Schalley, C. A. Chiroptical inversion of a planar chiral redox-switchable rotaxane. *Chem. Sci.* **10**, 10003-10009 (2019).

(33) Corra, S., de Vet, C., Groppi, J., La Rosa, M., Silvi, S., Baroncini, M. & Credi, A. Chemical On/Off Switching of Mechanically Planar Chirality and Chiral Anion Recognition in a [2]Rotaxane Molecular Shuttle. *J. Am. Chem. Soc.* **141**, 9129-9133 (2019).

(34) Martinez-Cuezva, A., Saura-Sanmartin, A., Alajarin, M. & Berna, J. Mechanically Interlocked Catalysts for Asymmetric Synthesis. *ACS Catalysis*, 7719-7733 (2020).

(35) Pairault, N. & Niemeyer, J. Chiral Mechanically Interlocked Molecules - Applications of Rotaxanes, Catenanes and Molecular Knots in Stereoselective Chemosensing and Catalysis. *Synlett* **29**, 689-698 (2018).

(36) Mitra, R., Zhu, H., Grimme, S. & Niemeyer, J. Functional Mechanically Interlocked Molecules: Asymmetric Organocatalysis with a Catenated Bifunctional Bronsted Acid. *Angew. Chem. Int. Ed.* **56**, 11456-11459 (2017).

(37) Pairault, N., Zhu, H., Jansen, D., Huber, A., Daniliuc, C. G., Grimme, S. & Niemeyer, J. Heterobifunctional Rotaxanes for Asymmetric Catalysis. *Angew. Chem. Int. Ed.* **59**, 5102-5107 (2020).

(38) Dommaschk, M., Echavarren, J., Leigh, D. A., Marcos, V. & Singleton, T. A. Dynamic Control of Chiral Space Through Local Symmetry Breaking in a Rotaxane Organocatalyst. *Angew. Chem. Int. Ed.* **58**, 14955-14958 (2019).

(39) Cakmak, Y., Erbas-Cakmak, S. & Leigh, D. A. Asymmetric Catalysis with a Mechanically Point-Chiral Rotaxane. *J. Am. Chem. Soc.* **138**, 1749-1751 (2016).